

**INTEGRATED BOULDER ANALYSIS AT NIGHTINGALE CAN INFORM SAMPLE RETURN FROM ASTEROID BENNU.** Erica R. Jawin<sup>1</sup>, R.-L. Ballouz<sup>3</sup>, H. H. Kaplan<sup>2</sup>, A. J. Ryan<sup>4</sup>, M. M. Al Asad<sup>5</sup>, J. L. Molaro<sup>6</sup>, and B. Rozitis<sup>7</sup>, <sup>1</sup>Smithsonian National Air and Space Museum, Washington, DC, USA ([jawine@si.edu](mailto:jawine@si.edu)), <sup>2</sup>Johns Hopkins APL, Laurel, MD, USA, <sup>3</sup>NASA Goddard, Greenbelt, MD, USA, <sup>4</sup>University of Arizona, Tucson, AZ, USA, <sup>5</sup>Brown University, Providence, RI USA, <sup>6</sup>Open University, Milton Keynes, UK.

**Introduction:** The surface sample of asteroid (101955) Benu is traveling towards Earth onboard the OSIRIS-REx spacecraft, scheduled to arrive in September 2023. Sample analysis plans are being developed based on investigations of orbital data which suggest there are two distinct rock types on Benu: dark, rugged boulders with low thermal inertia (TI) and high porosity; and bright, smooth boulders with higher TI and low porosity which also contain bright spots (carbonates) [1–3]—although morphologic assessments suggest there may be additional variation within these two categories, for a total of four groups [4].

To best prepare for the returned sample, we must more fully understand the diversity of boulders at a range of sizes on Benu. We are performing the largest investigation of Benu boulder properties to date, down to 2 m diameter in several locations, with the full suite of instrumentation onboard the OSIRIS-REx spacecraft [5]. This analysis includes initially assessing and classifying boulders based on physical properties and albedo using OCAMS and OLA data. Results are then used as inputs for chemical and thermophysical analyses using OVIRS and OTES data. Performing this integrated analysis of Benu's boulders will reveal their diversity and enable us to determine how many distinct boulder groups are present. This will provide insight into the parent body (or bodies) from which the rubble pile Benu was sourced. Investigations from different sites on Benu will reveal which, if any, boulder properties are due to recent processing on Benu, and which are due to parent body processes. Here we report on our analysis at the Nightingale region and present hypotheses for the returned sample.

**Data:** We use the Detailed Survey mosaic [6] for mapping and boulder identification, with a ground sample distance of 5 cm. We use the highest-resolution data from the Recon mission phase for our detailed analyses, including PolyCam (PC) images for morphologic assessment, OLA for surface roughness quantification, OVIRS for chemical analysis, and OTES for the thermophysical investigation. We also extracted albedo data from the PC normal albedo map [7] and color data from the MapCam color mosaic [1].

**Results:** We mapped ~400 boulders in the Nightingale region from 2 to 24 m diameter which have PC albedos ranging from 0.04 to 0.068 (**Figure 1**). Our morphologic analysis assessed characteristics including angularity, texture, and the presence of clasts, layers, and bright spots. We used these characteristics to assign

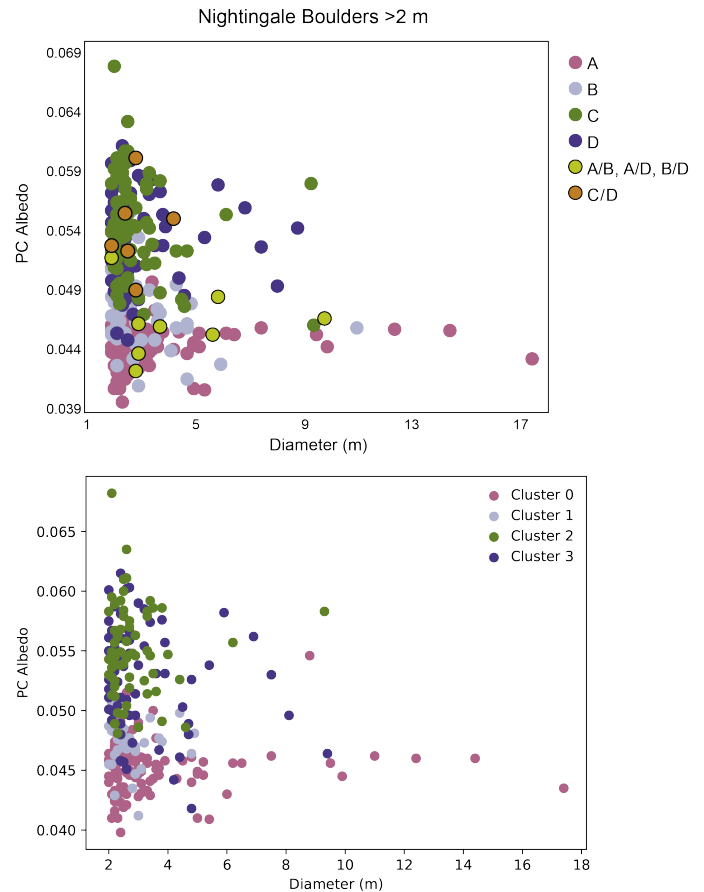


**Figure 1.** (Top) Diameter versus normal albedo based on our manual classification. (Bottom)  $k$ -prototypes clustering with four clusters. We did not include mixed type (e.g., A/B) boulders in the clustering algorithm.

each boulder to one of four morphologic types which were developed from previous analyses [4] (**Table 1**), and those same characteristics hold for the boulders in Nightingale: Type A boulders are on average the lowest albedo, 0.045, contain visible clasts ~10 cm and larger, and can contain layering in the matrix. Type B boulders have a similar mean albedo but are slightly smoother in texture than Type A and generally lack clasts, layers, or bright spots. Type C boulders have higher mean albedo, 0.055, are distinctly angular and smooth with no clasts or layers, and can contain bright spots. Type D boulders have similar mean albedo to Type C but with slightly rougher texture, and contain bright spots. The most distinct boulder morphologies are Types A and C, while Types B and D can be difficult to distinguish at small scales. Contacts between different morphologic types

are present on ~5% of boulders with the most common contacts between Type A and B, with fewer examples showing C and D; A and D; and B and D (**Figure 1**).

Manual Classification	Morphology	PC Albedo
A	Rounded Rugged Clasts present Layers present	$0.045 \pm 0.002$
B	Subrounded Intermediate texture	$0.047 \pm 0.002$
C	Angular Smooth Bright spots present	$0.055 \pm 0.004$
D	Subrounded Intermediate texture Bright spots present	$0.054 \pm 0.004$

**Table 1.**

As validation for our manual boulder classification into Types A-D, we implemented two statistical clustering algorithms: *k*-modes (for categorical data) and *k*-prototypes (for mixed categorical and numeric data) [8] to automatically sort our morphologic and albedo data into an unspecified number of clusters that minimize matching dissimilarity within the clusters. We then compared the results to our manual analysis. Both the *k*-modes (for morphologic data) and *k*-prototypes (for morphologic and albedo data) implementations generated four boulder clusters with centroids that matched our manual classification almost exactly.

We are in the process of measuring the RMS roughness from several transects across each boulder at multiple baselines in order to extract the Hurst exponent, *H*, and compare differences in roughness with scale. We find that Type A boulders are the roughest at all scales, while Type B and D boulders are the smoothest at small and large scales, respectively. A portion of the boulders have a natural breakpoint in the Hurst exponent. Similar breaks have been identified on lunar surfaces which usually denote a change in the major geologic process controlling roughness at that scale [9]. For boulders on Bennu, this could distinguish processes inherited from Bennu's parent body versus later evolution on Bennu. Additional investigations of *H* breakpoint with boulder type are ongoing.

Our initial thermal analysis involved calculating mapped boulder abundance and normal albedo in each Recon A OTES spot, which are compared to corresponding spot TI values obtained with the thermal model and methods of [2]. Preliminary results (**Figure 2**) show a correlation between albedo and TI where low albedo boulders (Type A, B) have lower TI, and high albedo boulders (Type C, D) have high TI, in agreement with previous studies [2].

**Discussion:** The high degree of agreement between our manual boulder classification and the automated clustering implies the four boulder groups we defined are robust and distinct (**Table 1**). This could imply that instead of only two dominant lithologies on Bennu as proposed [1–3], there are four populations with distinct origins and evolutionary pathways. These four populations could correspond to distinct regions on the same parent body, perhaps at various depths; conversely, some or all of the boulder groups could have originated on different parent bodies which were fragmented and mixed on Bennu. Given morphologic contacts found between different boulder types, we favor the former model of one heterogeneous parent body. We therefore hypothesize that the returned sample will be diverse in texture and albedo following **Table 1**, as well as in TI, but will show isotopic variations consistent with a single initial reservoir of material. Additionally, we suggest that potentially weak Type A and B boulders may have preferentially disaggregated during TAG and in the Sample Return Canister during Earth Return. Further insight into the boulder diversity at Nightingale will continue as we incorporate the full spectral and thermal analysis into our classification, and as we expanding our analysis to other regions on Bennu we can determine how representative the returned sample is of Bennu globally.

**Acknowledgments:** This work is supported by NASA NFDAP Grant # 80NSSC21K0827.

**References:** [1] DellaGiustina et al., (2020) *Science*. **370**, eabc3660. [2] Rozitis et al., (2020) *Sci. Adv.* **6**, eabc3699. [3] Kaplan et al., (2020) *Science*. **370**, eabc3557. [4] Jawin et al., (2022) *53<sup>rd</sup> LPSC*, Abs. 2066. [5] Lauretta et al., (2017) *Space Sci. Rev.* **212**, 925–984. [6] Bennett et al., (2021) *Icarus*. **357**, 113690. [7] Golish et al., (2021) *Icarus*. **355**, 114133. [8] Huang, (1998) *Data Min. Knowl. Discov.* **2**, 283–304. [9] Rosenberg et al., (2011) *JGR*. **116**.

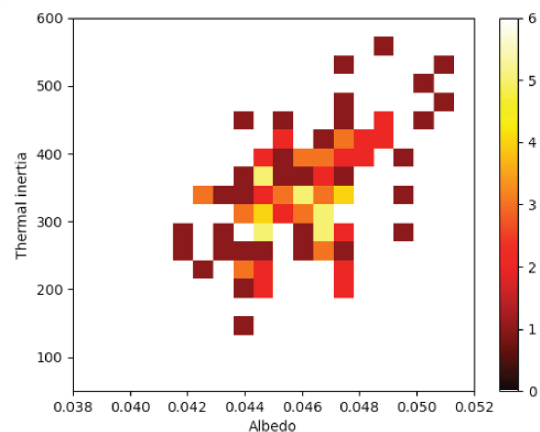


**Figure 2.** 2D histogram of PC normal albedo vs TI ( $\text{W m}^{-2} \text{J}^{-1} \text{s}^{-1/2}$ ) for OTES spots with <25% mapped boulder coverage.